


# An Active-Site Guanine Participates in *glmS* Ribozyme Catalysis in Its Protonated State

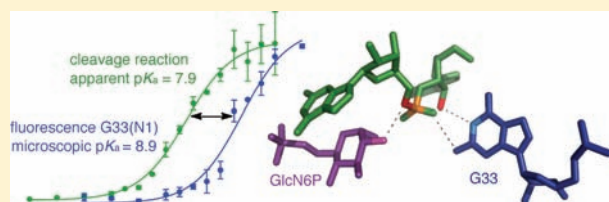
Júlia Viladoms,<sup>†</sup> Lincoln G. Scott,<sup>‡</sup> and Martha J. Fedor<sup>\*,†</sup>

<sup>†</sup>Department of Chemical Physiology, Department of Molecular Biology, and The Skaggs Institute for Chemical Biology, The Scripps Research Institute, 10550 North Torrey Pines Road, La Jolla, California 92037, United States

<sup>‡</sup>Cassia LLC, Suite 214, 3030 Bunker Hill Street, San Diego, California 92109, United States

 Supporting Information

**ABSTRACT:** Active-site guanines that occupy similar positions have been proposed to serve as general base catalysts in hammerhead, hairpin, and *glmS* ribozymes, but no specific roles for these guanines have been demonstrated conclusively. Structural studies place G33(N1) of the *glmS* ribozyme of *Bacillus anthracis* within hydrogen-bonding distance of the 2'-OH nucleophile. Apparent  $pK_a$  values determined from the pH dependence of cleavage kinetics for wild-type and mutant *glmS* ribozymes do not support a role for G33, or any other active-site guanine, in general base catalysis. Furthermore, discrepancies between apparent  $pK_a$  values obtained from functional assays and microscopic  $pK_a$  values obtained from pH–fluorescence profiles with ribozymes containing a fluorescent guanosine analogue, 8-azaguanosine, at position 33 suggest that the pH-dependent step in catalysis does not involve G33 deprotonation. These results point to an alternative model in which G33(N1) in its neutral, protonated form donates a hydrogen bond to stabilize the transition state.



## INTRODUCTION

The *glmS* ribozyme is a unique catalytic RNA since it requires a cofactor for catalytic activity and it is also a riboswitch that regulates gene expression through cleavage upon binding D-glucosamine-6-phosphate (GlcN6P). It was discovered in the 5'-UTR of Gram-positive bacterial mRNAs that encode L-glutamine-D-fructose-6-phosphate amidotransferase, which generates GlcN6P, an important intermediate in sugar metabolism and cell wall biosynthesis.<sup>1–3</sup> High concentrations of GlcN6P trigger *glmS* ribozyme cleavage, generating a 5'-OH terminus that targets the mRNA for degradation,<sup>4</sup> thereby providing negative feedback regulation of the GlnS enzyme. The ligand-activated catalysis of the *glmS* ribozyme is the first example of a natural self-cleaving RNA that employs a coenzyme, which contributes chemical versatility that is otherwise not available with only four nucleotides.<sup>5</sup> As such, it is a good model for the study of RNA–ligand interactions, as well as catalytic chemistry performed by an RNA–cofactor complex.

The *glmS* ribozyme is one of the five small self-cleaving ribozyme motifs that catalyze site-specific intramolecular phosphodiester cleavage. The hairpin, hammerhead, hepatitis delta virus (HDV) and *Neurospora* Varkud satellite (VS) ribozymes were originally discovered in satellite RNAs, but recent studies show that ribozymes are broadly distributed in nature.<sup>6</sup> Small self-cleaving RNAs catalyze phosphate-transfer reactions involving nucleophilic attack of a 2'-oxygen on the adjacent phosphorus to create a trigonal-bipyramidal oxyphosphorane transition state. Breaking of the 5'-P–O bond generates a 5'-product (5'P) with a 2',3'-cyclic phosphate terminus and a 3'-product (3'P) with a 5'-OH terminus.<sup>6,7</sup> In this  $S_N2$ -type reaction, attacking and leaving groups

adopt in-line geometry and undergo inversion of configuration at the phosphorus center. The reaction is potentially reversible, as the 2',3'-cyclic phosphate can be a substrate for RNA-mediated ligation.<sup>7</sup> It has been demonstrated that some ribozymes, including the *glmS*, do not require divalent metal ions for catalysis,<sup>7–9</sup> evidence that the RNA itself plays a direct chemical role. As RNA has limited chemical functionality, several strategies likely combine to produce significant rate enhancements.<sup>10</sup>

The *glmS* ribozyme is comprised of a core region that includes the GlcN6P binding pocket and a peripheral domain connected to the core by an H-type pseudoknot.<sup>11,12</sup> The cofactor binds immediately adjacent to the scissile phosphate, with the substrate positioned for in-line attack in a preformed active site that does not undergo a major conformational change upon ligand binding.<sup>11,12</sup> Atomic resolution structures have shown that conserved guanines occupy virtually identical positions in the *glmS* (G33 in *Bacillus anthracis*, G40 in *Thermoanaerobacter tengcongensis*), hairpin (G8), and hammerhead (G12) ribozyme active sites.<sup>7</sup> In each case, G(N1) lies within hydrogen-bonding distance of the 2'-OH nucleophile, reminiscent of the  $\epsilon$ -amino group of histidine-12 in RNase A,<sup>13</sup> which catalyzes the same reaction and serves as a model of concerted general acid–base catalysis. Moreover, N2 of G33 in the *glmS* and G8 in the hairpin ribozymes form hydrogen bonds with *pro-S\_P* nonbridging oxygens of the scissile phosphate. G33 is critical for self-cleavage of the *B. anthracis glmS* ribozyme; it is universally conserved,<sup>1</sup> and

Received: August 10, 2011

Published: September 21, 2011

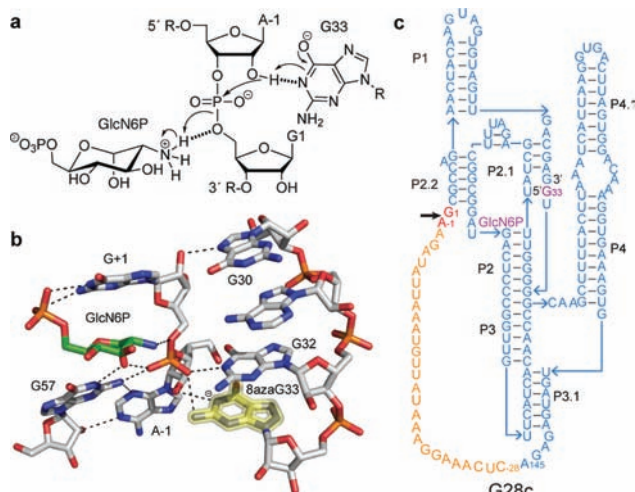


**Figure 1.** Sequence, structure, and function of the *glmS* ribozyme. (a) Proposed acid–base mechanism for the self-cleavage reaction catalyzed by the G33 and GlcN6P. (b) Model of the active-site structure showing the scissile phosphate and important guanine residues (based on the X-ray structure of the precleavage state of *B. anthracis glmS* with bound GlcN6P and 2'-OMeA-1, PDB entry 2NZ4,<sup>12</sup> with G8 replaced by 8azaG8 and the methyl group removed from the 2'-O of A-1 using PyMol).<sup>58</sup> (c) Sequence and secondary structure of the *glmS* ribozyme from *B. anthracis*. G28c is a circularly permuted variant used for kinetic and fluorescence experiments. A-1 and G1 (red) were mutated to C in the inactive ribozyme (G28cm).

its mutation to any other nucleotide inhibits cleavage almost completely.<sup>12,16</sup> But G33 does not seem well suited for the proposed role as a general base catalyst,<sup>12,16</sup> since the  $pK_a$  value for deprotonation of its N1 in solution is very basic ( $pK_a = 9.2$ ). However, RNA structures could shift the intrinsic ionization equilibria of nucleobase functional groups in either the acidic or basic direction,<sup>7,17</sup> and a sufficient fraction of the deprotonated form could be present at neutral pH to account for observed levels of catalysis even if the  $pK_a$  is not optimal.<sup>18</sup> Therefore, it is important to assess the proposed general acid–base catalysis model biochemically (Figure 1a).

Nucleobase ionization is important in RNA structure and also in RNA function when nucleobases participate in catalytic chemistry.<sup>17,19</sup> But methods used to probe nucleobase protonation states have been limited to RNA fragments or RNAs with inactivating modifications, which complicates the extrapolation of experimental results to functional RNAs. We recently developed a new method to monitor nucleobase protonation states directly in fully functional RNAs based on 8-azapurine fluorescence.<sup>20,21</sup> 8-Azaguanine (8azaG) is a guanine analogue that displays high fluorescence emission intensity when N1 is deprotonated (Figure 1b) and low fluorescence emission intensity when it is in the neutral, protonated form. This method provides a new approach to the analysis of proton-transfer steps in RNA-catalyzed reactions<sup>22,23</sup> that we have now applied to the *glmS* ribozyme for the first time.

We found that substitutions of G33 with A, C, or U perturbed the pH dependence of self-cleavage activity, but mutations of other active-site guanines did not. We also determined that the microscopic  $pK_a$  value for 8azaG33 ionization in a circularly permuted of the *B. anthracis glmS* ribozyme did not correlate well with the apparent  $pK_a$  value obtained from the pH dependence of cleavage kinetics. These results do not exclude a role for G33 in general acid–base catalysis, but they do indicate that G33

deprotonation is not responsible for the observed increase in activity with increasing pH. Our findings are consistent with models in which the neutral form of G33 donates a hydrogen bond to stabilize the transition state or participates in proton shuttling with GlcN6P.

## RESULTS

### Biochemical Characterization of the Natural *glmS* Ribozyme.

Many biochemical studies of *glmS* ribozymes have been performed using diverse divalent cation and activator concentrations, different buffering systems, and varied sequences and ribozyme configurations (*cis*- or *trans*-cleaving). Reported cleavage rates vary from 1 to 300  $\text{min}^{-1}$  in different systems.<sup>24,25</sup> Several atomic resolution structures of pre- and postcleavage states of *glmS* ribozymes have been reported, including wild-type and modified RNAs alone and in complexes with a variety of ligands.<sup>11,12,16,25,26</sup> We chose to work with the natural *glmS* ribozyme from *B. anthracis*,<sup>27</sup> identical in sequence to the *glmS* ribozyme of *Bacillus cereus*, because it is a well-characterized variant that cleaves virtually completely with reproducible, monophasic kinetics. Our wild-type construct, G18, comprises 161 nt from A-16 to A145 from the *glmS* mRNA of *B. anthracis*, with 18 nt upstream of the cleavage site (Figures 1c and S1a).

We first identified conditions under which observed cleavage kinetics monitor the cleavage step independently of metal or cofactor binding or product dissociation steps in the reaction pathway. The *glmS* ribozyme does not require direct coordination of divalent metal ions for catalytic chemistry, but they do promote catalysis by stabilizing the active structure and by coordinating the phosphate moiety of GlcN6P and assisting ligand binding.<sup>8,9,12</sup> The magnesium dependence of cleavage rates gave an affinity constant  $K_{1/2, \text{MgCl}_2} = 5.8 \pm 1.6 \text{ mM}$  (50 mM HEPES pH 7.5, 0.1 mM EDTA, 25 °C, 1 mM GlcN6P) (Figure S3c). GlcN6P bound with low affinity across a range of pH values, with approximate  $K_{d, \text{app, GlcN6P}} = 4 \text{ mM}$  at pH 5.5, 1 mM at pH values of 6.5, 7.5, and 8.5, and 2 mM at pH 9.5 (50 mM buffer, 0.1 mM EDTA, 50 mM  $\text{MgCl}_2$ , 25 °C) (Figure S3a), consistent with previously published values.<sup>25,28</sup> We used 50 mM  $\text{MgCl}_2$  and 10 mM GlcN6P in subsequent assays to ensure that GlcN6P and  $\text{Mg}^{2+}$  concentrations were saturating at all pH values.

We determined rate and equilibrium constants for each step in a minimal kinetic mechanism using pre-steady-state kinetics methods (Figure S2). Self-cleavage reactions typically proceeded to >90% completion, evidence of uniform ribozyme folding. The  $k_{\text{max}}$  value of  $191 \pm 5 \text{ min}^{-1}$  is among the highest determined for any *glmS* ribozyme.<sup>25</sup> *GlmS* ribozyme variants that have 3 nt (G3) or 18 nt (G18) (Figure S1a) upstream of the cleavage site exhibited virtually identical cleavage rates at pH 7.5 ( $97 \pm 19$  and  $93 \pm 5 \text{ min}^{-1}$ , respectively), evidence that no intermolecular interactions between 5' and 3' cleavage products stabilize a product complex and slow dissociation. Therefore,  $k_{\text{max}}$  values likely monitor the cleavage step under these conditions.

We prepared an extended ribozyme that contained the entire 68-nt 5'-UTR of the *glmS* mRNA (G68, Figure S1a) to investigate whether upstream sequences participate in unrecognized tertiary interactions with the core, as has been the case for other ribozymes.<sup>7</sup> We could not detect any association of 5' and 3' cleavage products in native gels at RNA concentrations as high as 9  $\mu\text{M}$  (5'P:3'P 5:1, 4 °C). Weak product binding would favor rapid dissociation and prevent religation, which is consistent with our failure to observe the increased cleavage rates and lower cleavage extents expected for a pseudo-first-order reaction that reaches equilibrium between cleavage and ligation.<sup>29</sup> Moreover,

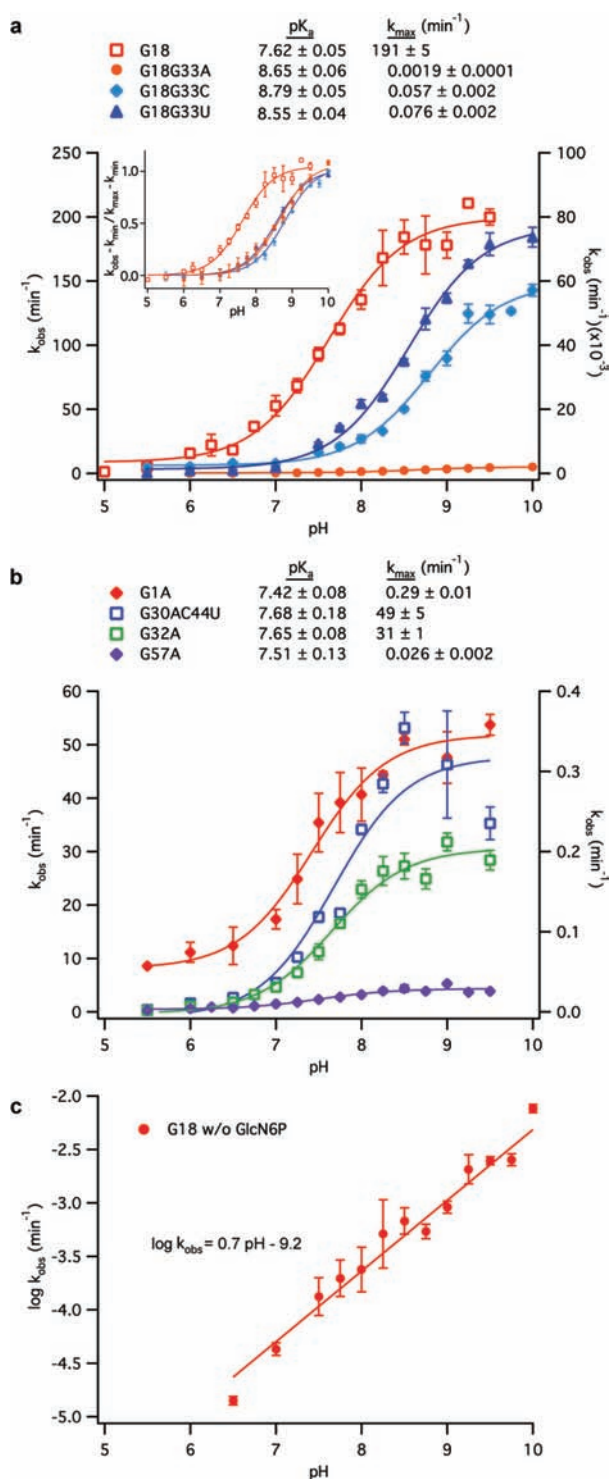


**Figure 2.** pH dependence of cleavage kinetics. (a) Cleavage kinetics of the wild-type *glmS* ribozyme (G18) and mutants G33A, G33C, and G33U in the presence of 10 mM GlcN6P. (b) Cleavage kinetics of the wild-type *glmS* ribozyme (G18) and mutants G1A, G30AC44U, G32A, and G57A in the presence of 10 mM GlcN6P. (c) Cleavage kinetics of G18 in the absence of GlcN6P.

the extended *glmS* ribozyme did not exhibit reduced  $\text{Mg}^{2+}$  dependency ( $K_{1/2, \text{MgCl}_2} = 10.5 \pm 4.7$  mM) (Figure S3c) or stronger cofactor binding affinity ( $K_{d, \text{app}, \text{GlcN6P}} = 1.5 \pm 0.1$  mM) (Figure S3b) relative to the truncated form at pH 7.5.

The GlcN6P cofactor and G33 are both essential for catalysis. The wild-type G18 ribozyme in the absence of GlcN6P and the G33A mutant ribozyme in the presence of GlcN6P both cleave at a rate near  $10^{-4} \text{ min}^{-1}$  at pH 7.5, only 10-fold faster than the uncatalyzed alkaline hydrolysis under the same experimental conditions.<sup>30</sup> Self-cleavage of G33A mutant ribozyme in the absence of GlcN6P could not be distinguished from background hydrolysis.

**pH Dependence of Cleavage Kinetics for Wild-Type and Mutant *glmS* Ribozymes.** At saturating concentrations of GlcN6P and magnesium, the pH dependence of self-cleavage kinetics for G18 fits well to an equation with a single ionizable group to give an apparent  $pK_a = 7.62 \pm 0.05$  (Figure 2a). This value falls within the range of previously reported ones.<sup>8,24,25,31</sup> In the absence of GlcN6P, the same ribozyme exhibits a log-linear pH–rate profile between pH 6.5 and 10 (Figure 2c).

G33 was substituted with each of the other natural bases (H = A, C, or U) to probe its role in catalytic chemistry. All of these mutations decreased cleavage rate constants by more than 2500-fold at pH 7.5, with the G33A mutation being particularly deleterious (Figure 2a). Rates were somewhat faster than those previously reported for similar mutants, but generally agreed within 40-fold.<sup>12,16</sup> These mutants exhibited very low activity across the entire pH range, but rates increased 20–70-fold between pH 5.5 and 10.0, similar to the wild-type ribozyme. pH–rate profiles could be fit to a simple Henderson–Hasselbalch equation to give apparent  $pK_a$  values of 8.65, 8.79, and 8.55 for G33A, G33C, and G33U mutants, respectively, which are slightly more basic than the apparent  $pK_a$  for the wild-type ribozyme.

**A *glmS* Ribozyme Variant with a Unique 8azaG Substitution in the Active Site.** Evaluating the role of the active-site G33 nucleobase using the fluorescent analogue 8azaG<sup>21,22</sup> required a *glmS* ribozyme variant with a unique 8azaG33 substitution. We designed a circularly permuted *glmS* ribozyme with G33 at the 5'-end (G28c, Figure 1c), which allowed us to incorporate a single 8azaG modification by priming transcription with 8-azaguanosine-5'-monophosphate (8azaGMP) in reactions that also contained the four natural nucleotide triphosphates (NTPs). The 32-nt linker, joining the natural A145 at the 3'-end to C-28 at the 5'-end, was designed to be long enough to allow the ribozyme to fold properly, based on the distance between 5'- and 3'-ends of the natural *glmS* ribozymes obtained from X-ray structures ( $\sim 57$  Å between 3'-OH A141 and 5'-OH A-1).<sup>12,25</sup> The initial construct exhibited multiphasic kinetics attributable to 3'-end heterogeneity. We inserted a 39-nt sequence downstream of the ribozyme that formed a 13-bp hairpin substrate for M1 RNA cleavage, which left homogeneous 3'-OH termini (Figure S4).<sup>32</sup> For control experiments, we prepared the unmodified circularly permuted ribozyme with a 5'-monophosphate (G28c) by priming transcription reactions with GMP, as described previously.<sup>23</sup> Increasing concentrations of GMP reduced incorporation of  $\gamma$ -<sup>32</sup>P-GTP at the 5'-end to about 10% in transcription reactions with 8 mM GMP and 4 mM NTPs, from which we inferred that GMP was incorporated at the 5'-end of 90% of the transcripts. The G28c *glmS* ribozyme with uniform 3'-termini exhibited monophasic kinetics similar to the wild-type ribozyme and comparable pH dependence ( $pK_{a, \text{app}} = 7.72 \pm 0.07$ ,  $k_{max} = 49 \pm 2 \text{ min}^{-1}$ , Figure 3a). Circular permutes with different linker lengths (29–34 nt) exhibited the same  $k_{cleav}$  values at pH 7.5 (Figure S5), indicating that the linker did not interfere with *glmS* ribozyme folding or catalysis. 8azaGMP was recognized by T7 RNA polymerase and incorporated in the first position with lower yields than GMP (50–80%). Transcription reactions with 2 mM NTPs and 25 mM 8azaGMP produced maximal

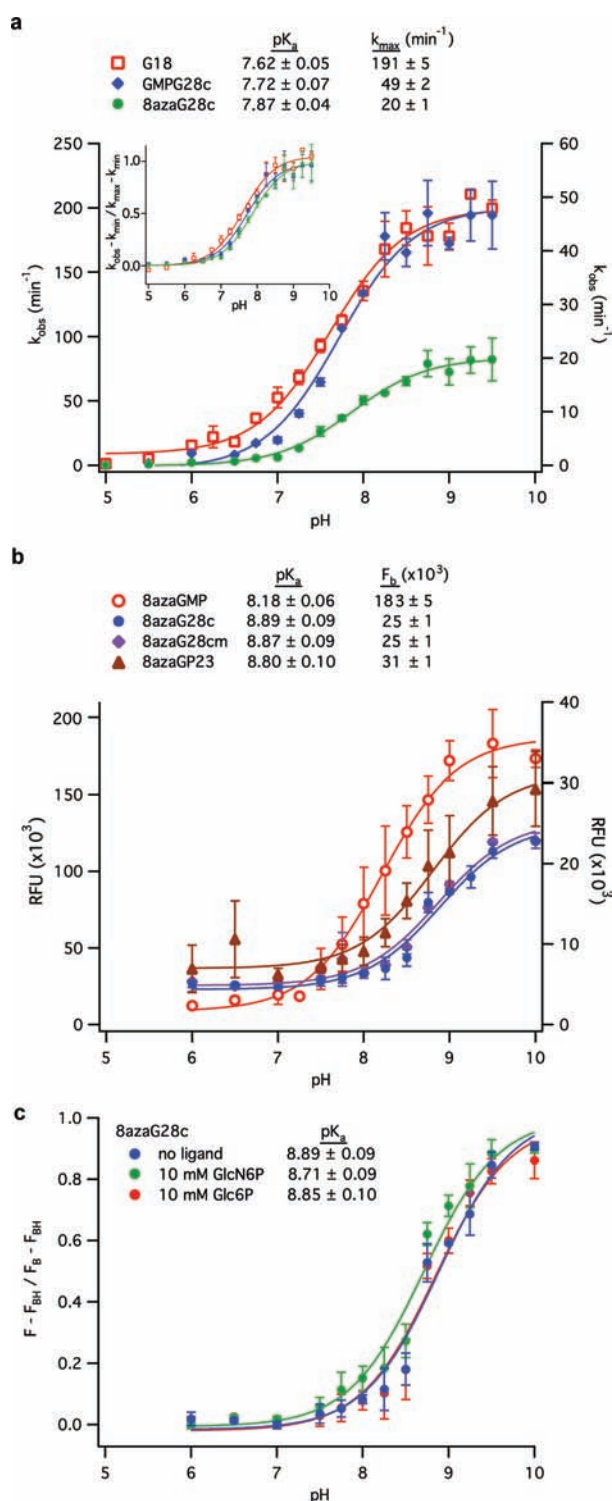


**Figure 3.** pH dependence of cleavage kinetics and 8-azaguanine fluorescence emission intensity. (a) Cleavage kinetics of the natural *glmS* ribozyme (G18), the circular permute (G28c), and a ribozyme with 8azaG at position 33 (8azaG28c) in the presence of 10 mM GlcN6P. (b) Fluorescence emission of 8azaGMP, active (8azaG28c) and inactive (8azaG28cm) ribozymes, and a *glmS* ribozyme fragment (8azaGP23) with no ligand. (c) Fluorescence emission of 8azaG28c with no ligand, with 10 mM GlcN6P cofactor, or with 10 mM Glc6P inhibitor.

8azaGMP incorporation without significantly compromising yields.

Initial attempts to ligate the 5'-terminal G33 to the 3'-terminal G32 using T4 RNA or DNA ligases were unsuccessful. Furthermore, the 3'-end was difficult to label in reactions with T4 RNA ligase and  $[5'-^{32}\text{P}]\text{pCp}$ , suggesting that it was inaccessible. Fortunately, the circularly permuted ribozyme (G28c) behaved similarly to the natural variant even without a covalent bond between G32 and G33, exhibiting only a 4-fold reduction in  $k_{max}$ . Substitution of G33 for 8azaG decreased  $k_{max}$  2-fold further, reduced cleavage extents by 15%, and shifted the apparent  $pK_a$  slightly in the basic direction ( $pK_{a,app} = 7.87 \pm 0.04$ ) (Figure 3a).

**8azaG Ionization Equilibria in the Ribozyme Active Site.** Fluorescence emission intensity depends on whether 8azaG (N1) is protonated or not, so microscopic  $pK_a$  values for 8azaG deprotonation can be determined from pH–fluorescence profiles. Fluorescence assays of 8-azaguanine (8azaG), 8-azaguanosine, 8azaGTP, and 8azaG-oligoribonucleotides in single-stranded form and in perfectly paired and bulged duplexes have shown that 8azaG deprotonation is significantly less favorable in the context of an oligonucleotide or structured RNA than in the free nucleobase or 8azaGTP.<sup>21,33</sup>

In the present study, we determined microscopic  $pK_a$  values for 8azaG deprotonation under the same conditions used for the analysis of *glmS* ribozyme activity (Figure 3b). Incorporation of 8azaG into single-stranded (8azaGP23, Figure S1b) and folded RNAs (8azaG28c and 8azaG28cm, Figure 1c) shifted  $pK_a$  values for 8azaG deprotonation in the basic direction and decreased, as expected, fluorescence intensity relative to 8azaGMP in solution, especially in highly structured RNAs.

We measured a microscopic  $pK_a$  value of  $8.9 \pm 0.1$  for deprotonation of 8azaG33 in the *glmS* ribozyme active site. This value is significantly (Welch *t* test,  $P < 0.01$ ) more basic than the apparent  $pK_a$  value of  $7.9 \pm 0.1$ , calculated from the pH dependence of 8azaG28c cleavage kinetics under the same conditions, with a  $\Delta pK_a$  of  $1.0 \pm 0.2$ .

**Ligand Effects on Microscopic  $pK_a$  Values.** A mutationally inactivated ribozyme variant 8azaG28cm (bearing A-1C and G1C mutations) and a short, unstructured RNA (8azaGP23) exhibited the same pH–fluorescence profile in the presence of GlcN6P or D-glucose-6-phosphate (Glc6P), at concentrations ranging from 10  $\mu\text{M}$  to 10 mM, as in their absence. Fluorescence of the active 8azaG28c ribozyme did not change when Glc6P was added, but addition of GlcN6P produced a very slight but statistically significant shift (Welch *t* test,  $P < 0.05$ ) (Figure 3c).

**Influence of Other Active-Site Guanines on Apparent  $pK_a$  Values.** Several active-site guanines other than G33 are highly conserved (G1, G30, G32, and G57,  $\geq 97\%$ ),<sup>14</sup> and mutation of these residues severely impairs *glmS* ribozyme activity.<sup>26,34</sup> Atomic resolution structures suggest that these guanines contribute to ribozyme function by forming hydrogen bonds that stabilize active-site architecture and align the reactive 5'- and 2'-oxygens with phosphorus (Figure 1b).<sup>11,12,26</sup>

We examined the effects on activity and pH dependence for *glmS* ribozymes in which these guanines were replaced by nucleobases with different acid–base properties and H-bonding patterns. If the protonation state of one of these guanines were responsible for a pH-dependent step in catalysis, substitution with nucleobases that have different intrinsic  $pK_a$  values would have corresponding effects on the pH–rate profiles. However, G-to-A mutations at these positions (G1A, G30AC44U, G32A, and G57A) did not shift apparent  $pK_a$  values significantly (Figure 2b), indicating that no active-site guanine is responsible for the pH-dependent catalytic step. Cleavage rates were notably slower for just two of the mutants, G1A ( $k_{max} = 0.29 \pm 0.01 \text{ min}^{-1}$ ) and G57A ( $k_{max} = 0.026 \pm 0.002 \text{ min}^{-1}$ ).

## DISCUSSION

It was crucial to establish a kinetic framework for mechanistic studies of the *glmS* ribozyme that would enable us to distinguish pH effects on  $k_{\text{cleav}}$  and  $K_{\text{d,GlcN6P}}$  values from effects on divalent metal binding, RNA folding, ligation, or product dissociation steps in the reaction pathway. The self-cleaving *glmS* ribozyme from *B. anthracis*<sup>27</sup> exhibited maximum rates approaching  $200 \text{ min}^{-1}$  in reactions with saturating concentrations of GlcN6P and  $\text{MgCl}_2$ , comparable to the fastest rates reported for *glmS* ribozymes.<sup>25</sup> Since longer products would be expected to dissociate more slowly and ribozymes with 3-nt (G3) or 18-nt (G18) 5' cleavage products cleaved at virtually identical rates, observed cleavage rates did not appear to reflect slow product dissociation. The  $k_{\text{cleav}}$  value measured at pH 7.5 was at least  $10^7$ -fold faster than noncatalyzed cleavage under the same conditions<sup>30</sup> and only 7–8-fold slower than the fastest VS and hammerhead ribozyme rates.<sup>19</sup> The *glmS* ribozyme likely combines several catalytic strategies to achieve these high rates.<sup>10</sup>

Binding of GlcN6P was weak, with  $K_{\text{d,app}}$  values in the millimolar range at all pH values tested, consistent with other recent reports.<sup>25,28</sup> Much lower values ( $K_{\text{d}} \approx 200 \mu\text{M}$ ) reported in earlier studies<sup>2,34</sup> likely reflected RNA folding.<sup>28</sup> Weak binding can be explained in part by the fact that GlcN6P equilibrates rapidly in solution between two cyclic anomers ( $\alpha$  and  $\beta$ ) in a ratio that depends on pH, with the  $\alpha$ -anomer predominating at low pH and the  $\beta$ -anomer at high pH.<sup>35</sup> The ribozyme selectively binds the  $\alpha$ -axial anomer, with  $K_{\text{d}} = 0.4 \text{ mM}$  at pH 7.5, as determined recently using NMR,<sup>35</sup> and suggested earlier from crystal structures of ribozyme complexes.<sup>12,16,25,26</sup> The apparent binding affinity for the anomeric mixture has been calculated to be  $0.8 \text{ mM}$  at pH 7.5,<sup>35</sup> similar to the results reported here. A high  $K_{\text{d,app}}$  value for GlcN6P binding might be appropriate for the physiological concentration at which negative feedback regulation of GlcN6P synthesis is required. The affinity of the ribozyme for GlcN6P increases with pH, with a modest reduction above pH 9. This behavior might be related to the cofactor's two ionizable groups: the primary amine and the phosphate moiety. The  $\text{p}K_{\text{a}}$  of the GlcN6P amino group is 8.1–8.2 in solution.<sup>24,36</sup> Recent studies have established that binding to the active site perturbs its  $\text{p}K_{\text{a}}$  value to about 7.<sup>35,36</sup> The intrinsic acidity of the phosphate moiety is also perturbed toward neutrality in the active site to a value of 6.4.<sup>36</sup> It appears then that the ribozyme preferentially binds the amine form of GlcN6P.<sup>36</sup> Protonation of the amine group would be responsible for diminished binding affinity at low pH, consistent with indirect evidence that GlcN6P binding is pH-dependent while Glc6P is not,<sup>26</sup> and as previously proposed in a computational study.<sup>37</sup> Conversely, another computational study indicated that the ammonium form binds preferentially to the active site at physiological pH, with the phosphate group being responsible for low binding affinity at acidic pH values, since binding of the monoprotonated form is weaker.<sup>38</sup> This model was supported by experimental evidence that the pH dependence of cofactor binding correlates with the  $\text{p}K_{\text{a}}$  of the GlcN6P phosphate moiety in solution,<sup>9,25</sup> although it is perturbed in the active site toward neutrality.<sup>36</sup> The intrinsic acidities of both the amino and phosphate groups of bound GlcN6P<sup>36</sup> are close to the apparent  $\text{p}K_{\text{a}}$  of binding and could contribute to reduced affinity at low pH.

Phylogenetic comparisons revealed conserved sequences upstream of the cleavage site,<sup>2</sup> reminiscent of extended forms of hairpin and hammerhead ribozymes in which peripheral interactions stabilize functional structures but are not essential for activity. The

enhanced tertiary structure stability conferred by peripheral sequences reduces  $\text{Mg}^{2+}$  dependency relative to minimal ribozymes and makes extended ribozymes more efficient RNA ligases.<sup>7</sup> However, a *glmS* ribozyme variant with the entire mRNA upstream sequence (G68) was not detectably different from the truncated form (G18). No stable cleavage product complexes were detected in native gels, and cleavage reactions did not show the accelerated rates and lower extents that would be expected for a ribozyme that catalyzes religation of bound products. Thus, the *glmS* ribozyme is more like the HDV ribozyme than the hammerhead or hairpin ribozymes; despite the microscopic reversibility of the phosphodiester transesterification reaction, the 5'-cleavage product dissociates rapidly after cleavage and it does not function as an RNA ligase.

The apparent  $\text{p}K_{\text{a}}$  value of 7.6 that we measured for cleavage of the *glmS* ribozyme–GlcN6P complex falls between values from 7.5 to 7.8 reported previously.<sup>8,24,25,31</sup> Recently a lower value of 6.9 was reported when taking into account the fraction of  $\alpha$ -anomer present at each pH.<sup>35</sup> Apparent  $\text{p}K_{\text{a}}$  values for each of the G33-to-H mutant ribozymes were shifted by approximately 1 unit in the basic direction. If the pH dependence of cleavage reflected the ability of G33(N1) to function as a general base catalyst by removing a proton from the nucleophilic 2'-OH, the apparent  $\text{p}K_{\text{a}}$  of the reaction would be expected to shift according to the microscopic  $\text{p}K_{\text{a}}$  of the nucleobase at position 33. Our results do not support this model because the microscopic  $\text{p}K_{\text{a}}$  values for deprotonation of adenosine, cytosine, and uridine range from 3.5 to 9.2, but the apparent  $\text{p}K_{\text{a}}$  for ribozyme cleavage shifted uniformly in the basic direction. The wild-type ribozyme cleavage rates displayed log-linear pH dependence with a slope near 1 in the absence of cofactor, consistent with a rate-determining step that involves deprotonation of a functional group with a  $\text{p}K_{\text{a}}$  significantly above 10, such as water.<sup>39</sup> Alternatively, the log-linear pH dependence could also reflect ionization of G33(N1) if the microscopic  $\text{p}K_{\text{a}}$  of G33 was shifted above 10 in the active site of the aporibozyme. However, this does not seem to be consistent with our fluorescence measurements that gave microscopic  $\text{p}K_{\text{a}}$  values below 8.9 for 8azaG33 in the ribozyme active site.

Although G33 deprotonation is not responsible for the increase in activity with increasing pH, G33 mutations do affect apparent  $\text{p}K_{\text{a}}$  values. These values seem to correlate with the intrinsic basicity of the activator,<sup>24</sup> evidence that GlcN6P contributes to the pH dependence of the rate-limiting step. The correspondence between the apparent  $\text{p}K_{\text{a}}$  value obtained from pH–rate profiles and the microscopic  $\text{p}K_{\text{a}}$  for deprotonation of the amine of GlcN6P is even closer in view of the fact that the  $\text{p}K_{\text{a}}$  for protonation of the bound ligand is lowered to 7.3 in the active site.<sup>36</sup> Tuning of the  $\text{p}K_{\text{a}}$  of bound ligand by G33 would account for the effects of G33H mutations on the pH dependence of cleavage kinetics. This result is consistent with Raman crystallography measurements of the  $\text{p}K_{\text{a}}$  of the GlcN6P amine moiety, which decreased by 0.8 unit in the wild-type ribozyme inactivated by a 2'-deoxy substitution at the cleavage site but was not altered in the G40A (G33A) mutant.<sup>36</sup>

Circularly permuted ribozymes with 5'-terminal GMP or 8azaGMP exhibited a 4–8-fold loss of activity, perhaps because the G32–G33 phosphodiester bond is needed for optimal alignment of reacting groups. Thus, 8-azaguanine reports on the ionization state of a close guanine analogue in a functional active site. Notably, the microscopic  $\text{p}K_{\text{a}}$  value for 8azaG ionization in the active site was not shifted toward neutrality to correspond with the apparent  $\text{p}K_{\text{a}}$  value determined from the pH dependence of reaction kinetics. Rather, it was perturbed in the basic direction.

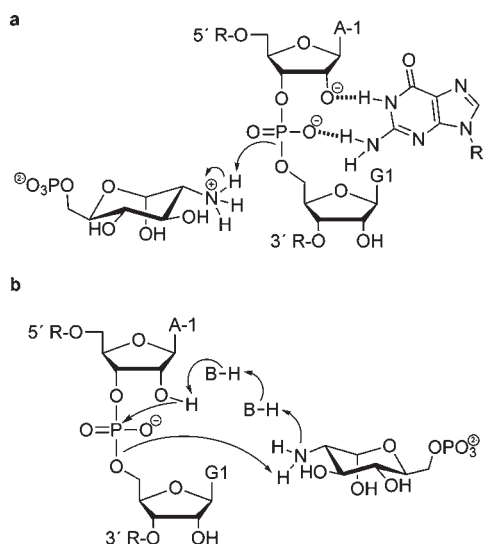


**Figure 4.** Catalytic models for *glmS* ribozyme cleavage. (a) Model in which G33 acts as hydrogen bond acceptor, facilitating specific base catalysis by a water or hydroxide molecule, and GlcN6P acts as the general acid catalyst. (b) Model in which GlcN6P acts as a general base catalyst, through tightly bound water or other active-site groups, and also as a general acid catalyst.

8azaG ionization equilibria were similar in the active ribozyme, an unstructured fragment, and a mutationally inactivated ribozyme. Small differences arose, however, in active ribozyme–ligand complexes, which exhibited minor acidic shifts. This effect could reflect a subtle difference in the environment of 8azaG33 in pre- and postcleavage states.

There is a modest but clear discrepancy between the pH dependence of *glmS* ribozyme activity and 8azaG33 deprotonation, arguing against the idea that deprotonation of G33(N1) is responsible for the pH-dependent transition in catalytic activity. This finding is consistent with the absence of the acidic shift in the apparent  $pK_a$  of the G33A mutant that would be expected if the residue at position 33 were responsible for the pH-dependent step due to the difference in intrinsic basicity between A(N1) and G(N1). These results do not rule out the possibility that G33 participates in *glmS* catalytic chemistry, but the simplest interpretation is that the neutral, protonated form of G33 contributes to catalysis by donating hydrogen bonds that provide electrostatic stabilization of the transition state and help to position reactive groups for the in-line attack mechanism (Figure 4a). Consistent with this model, a computational study suggested that deprotonated G33 is incompatible with *glmS* active-site architecture.<sup>38</sup>

The *glmS* ribozyme is unique among ribonucleases, protein, or RNA in requiring both G33 and GlcN6P for catalysis; either moiety in isolation provides negligible rate acceleration. This cooperativity implies that G33 and GlcN6P influence the chemical properties of the other and that the mechanism is more complex than general acid and base catalysts operating in an independent manner.<sup>16,40,41</sup> In contrast, mutation of the residues that act as general base and general acid in RNase A (His12 and His119) reduce cleavage rates by 700 000- and 400 000-fold, respectively, combining to give a total rate enhancement of  $10^{11.13}$ . Likewise, 850- and 14 000-fold rate enhancements contributed by G8 and A38 of the hairpin ribozyme, respectively, combine to produce a total rate enhancement of  $10^{7.7}$ . Recent studies suggest that the identity of the residue at position 33 in

the *glmS* ribozyme modulates the microscopic  $pK_a$  of the amine group of GlcN6P,<sup>36,37</sup> and that GlcN6P and unprotonated G33 cannot be accommodated together in the active site.<sup>38</sup> How G33 modulates the catalytic power of GlcN6P, and vice versa, remains an open question. Direct interaction between the two moieties seems unlikely, since the distance from the amine of GlcN6P to G33(N1) is nearly 7 Å. G33 mutation might interfere with ligand binding and/or ionization by disrupting active-site architecture in a role analogous to that of G+1 in the hairpin ribozyme, which forms tertiary interactions that are critical for alignment of the reactive phosphodiester in the active site.<sup>42</sup> However, this model is inconsistent with evidence that wild-type and the G33A ribozyme structures are nearly the same.<sup>16,25</sup>

The role of the GlcN6P cofactor in the catalytic mechanism is also a key question. GlcN6P could be the general acid catalyst that protonates the departing 5'-O (Figure 4a). The protonated form of GlcN6P would also stabilize the negative charge that accumulates in the penta-oxygen transition state. A dual role for GlcN6P could explain the negligible activity of the aporibozyme. A proton relay model in which GlcN6P serves as both the general base and the general acid is also consistent with these results (Figure 4b). The unprotonated amino form of GlcN6P could act as the general base through tightly bound water and, once protonated, carry out electrostatic and general acid catalysis.<sup>11,40,41</sup> Proton transfer could involve other groups in the active site,<sup>40</sup> including G33(N1), to account for the observed cooperativity between G33 and GlcN6P.

Mutation of other important active-site guanines to adenine residues decreases  $k_{\text{cleav}}$  but does not alter apparent  $pK_a$  values relative to that of the wild-type ribozyme, arguing that no active-site guanines are involved in the pH-dependent step. G1 forms hydrogen bonds with the phosphate of GlcN6P, helping to discriminate between GlcN6P and GlcN.<sup>26</sup> G30(N7) is within H-bonding distance of the 2'-OH of G1.<sup>11,12</sup> Interference pattern analyses point to important contacts of the exocyclic amine and N7 of G30 for ribozyme structure, ligand binding, and catalysis,<sup>43</sup> yet the G30A mutant, with the compensating C44U mutation, is nearly as active as the wild-type ribozyme, emphasizing the need for complementary functional and structural studies. Despite the high degree of conservation, the G32-to-A mutation had little effect on activity. Both G32 and G57 help position the scissile phosphate through H-bonding to the nonbridging oxygens. G57 also makes the contacts G57(N2)–A1(N3) and G57(N1)–GlcN6P(OH1). G57A and G57C mutations had previously been shown to reduce ribozyme activity qualitatively.<sup>34</sup> With a 7500-fold reduced rate, the G57A mutant is more deleterious than any point mutation apart from G33A. The G57A mutant is an inactive ribozyme with a wild-type G33 nucleotide, which could be useful as a negative control in biochemical experiments. Further studies are needed to reveal how the combination of interactions made by G57 to A-1, the scissile phosphate, and the cofactor contributes to its importance. Taken together, these results show that these individual active-site guanines do not participate directly in catalytic chemistry and in general do not contribute significant rate acceleration. Even so, the network of H-bonding and stacking interactions involving these conserved guanines is likely to be essential for stabilizing the functional active-site architecture.

## CONCLUSIONS

Different ribozymes exhibit unique constellations of catalytic strategies, including positioning and orientation of reactive groups, acid–base catalysis, electrostatic catalysis, or ground-state

destabilization.<sup>7,10,19,44</sup> Despite similarities in active-site architecture, different families of self-cleaving RNAs adopt distinct global structures and exploit different ways of lowering the energy barrier to catalysis. Alignment of functional groups in the active site is a common strategy among self-cleaving ribozymes, but it can only account for part of the observed rate enhancements.<sup>45,46</sup> We show here that G33 of the *glmS* ribozyme behaves similarly to G8 of the hairpin ribozyme, providing essential interactions for orientation and positioning as well as electrostatic stabilization.<sup>22</sup> The main difference between the two ribozyme motifs lies in the large cooperativity between G33 and GlcN6P in *glmS* ribozyme activity, which contrasts with the independent contributions of G8 and A38 to hairpin ribozyme catalysis. Hammerhead and *Neurospora* VS ribozymes are also believed to use active-site guanines as general base catalysts to deprotonate the nucleophilic 2'-OH, whereas a hydrated Mg<sup>2+</sup> is proposed to act as a Lewis acid catalyst in the HDV ribozyme by forming an inner-sphere contact with the 2'-OH group.<sup>47</sup> It will be important to test these models by comparing microscopic and apparent pK<sub>a</sub> values for putative general base catalysts in these self-cleaving RNAs as well.

GlcN6P is proposed to serve as the general acid in the catalytic mechanism, with the microscopic pK<sub>a</sub> values of its amino and phosphate groups tuned toward neutrality in the active site of the *glmS* ribozyme.<sup>36</sup> The presence of a cofactor in a composite active site greatly expands the enzymatic repertoire of RNA, since coenzymes could provide additional chemical functionalities that would otherwise not be available in an all-RNA active site. Cytosine and adenine residues with perturbed pK<sub>a</sub> values and very similar positions accomplish the same role as GlcN6P in the HDV and hairpin ribozymes, respectively, while a 2'-OH and an adenine have been proposed to play this role in hammerhead and VS ribozymes, respectively. It is worth noting that, for the *glmS*, hairpin, and HDV ribozymes, it is the functional group associated with the departing 5'-O, and not with the 2'-OH nucleophile, that has a pK<sub>a</sub> shifted toward neutrality and is responsible for the pH dependence of the rate-determining step.<sup>7,23</sup> This evidence that stabilizing the developing charge on the 5'-O leaving group is particularly important for diverse self-cleaving ribozymes suggests that breaking the P–5'-O bond presents the highest energy barrier to catalysis of RNA self-cleavage.<sup>17,18</sup>

## EXPERIMENTAL SECTION

**Preparation of 8-Azaguanosine 5'-Monophosphate.** All chemicals were purchased from Sigma-Aldrich (St. Louis, MO) and used as received, unless otherwise specified. All enzymes were prepared from overexpressing strains as previously described, unless otherwise specified.

D-Ribose (0.3 g, 2.0 mmol) and 8-azaguanine (8azaG, 0.3 g, 2.0 mmol, MP Biomedicals) were dissolved in 0.2 L of synthesis buffer (0.0025 mM dATP, 0.1 mM kanamycin, 0.2 mM dAMP, 5 mM ampicillin, 10 mM MgCl<sub>2</sub>, 20 mM dithiothreitol, 50 mM potassium phosphate, 100 mM phosphocreatine, pH 7.5) at 37 °C. The synthesis was started with the addition of 50 units of adenylate kinase (*plsA*, EC 2.7.4.3) and 200 units of creatine phosphokinase (*ckmT*, EC 2.7.3.2, Sigma-Aldrich). The reaction was monitored by HPLC methods described elsewhere.<sup>48</sup> After 2 h, the conversion of dAMP to dATP appeared complete, and the synthesis of 8azaGMP was started with the addition of 10 units of ribokinase (*rbsK*, EC 2.7.1.15),<sup>49</sup> 15 units of 5-phospho-D-ribosyl- $\alpha$ -1-pyrophosphate synthetase (*prsA*, EC 2.7.6.1),<sup>50</sup> 20 units of xanthine-guanine phosphoribosyltransferase (*glyD*, EC 2.4.2.7),<sup>51</sup> and 25 units of inorganic pyrophosphatase (*hppA*, EC 3.6.1.1). After 72 h, when the

consumption of 8-azaguanine appeared unchanged, the reaction mixture was brought to 0.5 M ammonium bicarbonate, pH 9.5, and purified by boronate affinity chromatography<sup>52</sup> (1.6 mmol, 80% average isolated yield). The nucleotide analogue 8azaGMP was easily separated with >95% chemical purity, according to HPLC.

Characterization data: <sup>1</sup>H NMR (500 MHz, D<sub>2</sub>O)  $\delta$  5.99 (d, *J* = 4.8 Hz, 1H, H1'), 4.90 (dd, *J* = 5.1, 4.8 Hz, 1H, H2'), 4.47 (dd, *J* = 5.1, 4.8 Hz, 1H, H3'), 4.19 (ddd, *J* = 4.5, 4.8, 5.7 Hz, 1H, H4'), 3.83 (dd, *J* = 11.5, 4.5 Hz, 1H, H5'), 3.79 (dd, *J* = 11.5, 5.7 Hz, 1H, H5''); <sup>13</sup>C NMR (150 MHz, D<sub>2</sub>O)  $\delta$  159.0, 156.7, 152.6, 125.2, 88.9, 85.0, 73.5, 71.3, 64.8; HRMS (ESI-TOF) *m/z* [M+H]<sup>+</sup> calcd for C<sub>9</sub>H<sub>14</sub>N<sub>6</sub>O<sub>8</sub>P 365.0611, found 365.0608.

See RP-HPLC, UV, HRMS, <sup>1</sup>H NMR, and <sup>13</sup>C NMR characterization in Supporting Information Figures S6–S8.

**Preparation of RNAs.** The plasmid template used to transcribe the wild-type *glmS* from *B. anthracis* (pTG18) contains the 161 nt of the ribozyme sequence also present in pANX1, described elsewhere.<sup>6</sup> Briefly, it was prepared by Klenow extension of six overlapping primers and inserted into a pUC18 vector using *KpnI* and *SacI* restriction sites. Other plasmid templates (pTG3, pTG68, pTG18 mutants, pTG28ch, and pTG28chm) were prepared by QuikChange mutagenesis<sup>53,54</sup> of pTG18.

RNAs were prepared using T7 RNA polymerase transcription on 10 nM linearized plasmid templates (for G18, G68, G3, and G18 mutants)<sup>55</sup> or 50 nM PCR-amplified templates (for G28c and GP23).<sup>56</sup> Transcriptions were carried out at 37 °C for 2–4 h in 20 mM HEPES pH 8, 1 mM spermidine, 5 mM dithiothreitol, 0.01% Triton X-100, 4 mM NTPs, and 25 mM MgCl<sub>2</sub>. For the incorporation of 5'-guanosine monophosphate (GMP) or 8azaGMP in the first position of the transcript, reactions contained 4 mM NTPs and 8 mM GMP or 2 mM NTPs and 25 mM 8azaGMP, respectively. Incorporation ranged from 50 to 80% for 8azaGMP and was about 90% for GMP, as assessed by the decrease in the signal of  $\gamma$ -<sup>32</sup>P-GTP present in the reactions. For homogeneously labeled RNAs,  $\alpha$ -<sup>32</sup>P-ATP was added in the reactions at 1/10 of the total volume, and in some cases ATP concentration was decreased to 1 mM. The plasmids pTG18ch and pTG18chm contain the DNA template for transcription of G28c and G28cm, respectively, (Figure 1c) plus the sequence TAAGAG-GATCTGGTACCGAGCTCGAATT GAGGACG at the 3'-end. Following phenol–chloroform–isoamyl alcohol extraction and desalting by NAP column (GE Healthcare) or DEAE chromatography, G28ch and G28cm were cleaved with M1 RNA (5  $\mu$ M ribozyme RNA precursor, 100 nM M1 RNA, 50 mM HEPES pH 7.5, 100 mM NH<sub>4</sub>Cl, 0.1 mM EDTA, 75 mM MgCl<sub>2</sub>, 37 °C, overnight) to generate G28c and G28cm with homogeneous 3'-OH termini.<sup>32</sup> M1 RNA was prepared by in vitro transcription with T7 RNA polymerase of a PCR template amplified from *E. coli* genomic DNA.<sup>57</sup> RNAs were purified by denaturing gel electrophoresis and converted into sodium salts by DEAE-650M chromatography (Toyopearl).

**Self-Cleavage Kinetics.** Kinetic assays were performed on pre-folded RNAs, with saturating concentrations of MgCl<sub>2</sub> and GlcN6P, in order to avoid a slow folding step (*k*<sub>obs</sub> < 4 min<sup>-1</sup>) that could precede formation of the native structure capable of ligand binding and catalysis.<sup>25,28</sup> [ $\alpha$ -<sup>32</sup>P-ATP]-labeled RNA (5–20 nM) in 50 mM buffer (piperazine pH 5–6, PIPES pH 6–7, HEPES pH 7–8.25, HEPPS pH 8–9, CHES pH 8.75–10) and 0.1 mM EDTA was heated to 85 °C for 1 min, cooled to 25 °C, and then brought to a MgCl<sub>2</sub> concentration of 50 mM and incubated at 25 °C for 15 min. Reactions were started by addition of D-glucosamine-6-phosphate (GlcN6P) at saturating concentration of 10 mM, unless noted otherwise, in the same buffer solution. For self-cleavage rates below 1 min<sup>-1</sup>, cleavage was initiated by manually mixing 30  $\mu$ L of prefolded RNA with 30  $\mu$ L of GlcN6P in the same buffering system. At appropriate time points, 6  $\mu$ L aliquots were taken and quenched with 5 vol of 90% formamide, 50 mM EDTA, 0.1% bromophenol blue, and 0.1% xylene cyanol. Rates above 1 min<sup>-1</sup> were measured using a Rapid Quench System RQF-3 from KinTek Corp., where the driving solutions had the same composition as the reaction buffer.

Solutions of 200  $\mu\text{L}$  were prepared for both prefolded RNA and GlcN6P. Following manufacturer instructions for the use of the Rapid Quench System, samples were mixed in the reaction loop ( $\sim 14 \mu\text{L}$  of each) for each time point and collected onto 40  $\mu\text{L}$  of quenching buffer, for a total dilution of 1:5. Cleavage experiments were performed at 25  $^{\circ}\text{C}$ . Collected aliquots were fractionated on denaturing polyacrylamide gels. The fraction of cleaved ribozyme was quantified by radioanalytic imaging (PhosphorImager Storm 820 and ImageQuant software, Molecular Dynamics). Cleavage rate constants ( $k_{\text{cleav}}$ ) were calculated by fitting the fraction of cleaved product versus time to single-exponential eq 1:

$$f = f_0 + f_{\infty}(1 - e^{-k_{\text{cleav}}t}) \quad (1)$$

Apparent  $\text{p}K_{\text{a}}$  values were determined by fitting averaged data (from at least two replicates) to eq 2:

$$k_{\text{cleav}} = \frac{k_{\text{max}}}{1 + 10^{(\text{p}K_{\text{a}} - \text{pH})}} + k_{\text{min}} \quad (2)$$

Apparent dissociation constants ( $K_{\text{d,app}}$ ) and maximum rates at each pH ( $k_{\text{max}}$ ) were determined using eq 3:

$$k_{\text{cleav}} = \frac{k_{\text{max}}[\text{ligand}]}{[\text{ligand}] + K_{\text{M}}} \quad (3)$$

**Fluorescence Measurements.** Fluorescence was measured using a SpectraMax M2e plate reader (Molecular Devices). Solutions of 2  $\mu\text{M}$  8azaGMP or 5  $\mu\text{M}$  RNA (8azaG28c, 8azaG28cm, or 8azaGP23) were prepared in 50 mM buffer (as described above for kinetic studies) with 0.1 mM EDTA, heated to 85  $^{\circ}\text{C}$  for 1 min, and cooled to 25  $^{\circ}\text{C}$  before  $\text{MgCl}_2$  was added to 50 mM and samples were incubated at 25  $^{\circ}\text{C}$  for 15 min. Samples of 10  $\mu\text{L}$  each were added to 384-well black microplates (Greiner), excited at 290 nm and emission spectra were recorded between 330 and 450 nm, using a cutoff filter at 325 nm. Maximum absorption was at 365 nm. GlcN6P (purified by filtration through activated charcoal to eliminate residual UV absorption and fluorescence emission) or D-glucose-6-phosphate (Glc6P) buffered at the appropriate pH was added to a final concentration of 0.1, 1, 5, or 10 mM. Apparent  $\text{p}K_{\text{a}}$  values were determined by fitting the integrated fluorescence intensities between 330 and 450 nm to eq 4:

$$F = F_{\text{B}} + (F_{\text{BH}} - F_{\text{B}}) \frac{[\text{H}^+]}{K_{\text{a}} + [\text{H}^+]} \quad (4)$$

where  $F_{\text{B}}$  and  $F_{\text{BH}}$  are the fluorescence of deprotonated and protonated 8azaG, respectively, and  $K_{\text{a}}$  is the acid dissociation constant for protonation of N1 of 8azaG. Values reported are the mean and standard deviation of values obtained from two or more replicate experiments. Data were normalized using  $F_{\text{B}}$  and  $F_{\text{BH}}$  from fittings.

## ■ ASSOCIATED CONTENT

**Supporting Information.** Figure S1, sequences of the RNAs used in kinetic and fluorescence studies; Figure S2, minimal kinetic mechanism of *glmS* ribozyme self-cleavage; Figure S3, cofactor and  $\text{Mg}^{2+}$  binding data for G18 and G68 ribozymes; Figure S4, schematic preparation of G28c; Figure S5, cleavage kinetics for circular permuted ribozymes with different chain lengths; Figures S6–S8, characterizations of 8azaGMP. This material is available free of charge via the Internet at <http://pubs.acs.org>.

## ■ AUTHOR INFORMATION

### Corresponding Author

mfedor@scripps.edu

## ■ ACKNOWLEDGMENT

This work was supported by NIH grant RO1 GM046422 to M.J.F. We thank M. Saha, S. Grimm, and J. W. Cottrell for assistance with plasmid constructions, A. Ferretti from G. Joyce's laboratory for providing us with the PCR template for M1 RNA transcription, and J.W.C. and Peter Watson for critical reading of the manuscript. We also acknowledge J.W.C.'s help in acquiring the pH–rate profile for the G33U mutant and a replicate for G30AC44U and G1A mutants.

## ■ REFERENCES

- (1) Barrick, J. E.; Corbino, K. A.; Winkler, W. C.; Nahvi, A.; Mandal, M.; Collins, J.; Lee, M.; Roth, A.; Sudarsan, N.; Jona, I.; Wickiser, J. K.; Breaker, R. R. *Proc. Natl. Acad. Sci. U.S.A.* **2004**, *101*, 6421.
- (2) Winkler, W. C.; Nahvi, A.; Roth, A.; Collins, J. A.; Breaker, R. R. *Nature* **2004**, *428*, 281.
- (3) Milewski, S. *Biochim. Biophys. Acta* **2002**, *1597*, 173.
- (4) Collins, J. A.; Irnov, I.; Baker, S.; Winkler, W. C. *Genes Dev.* **2007**, *21*, 3356.
- (5) Cochrane, J. C.; Strobel, S. A. *RNA* **2008**, *14*, 993.
- (6) Ferré-D'Amaré, A. R.; Scott, W. G. *Cold Spring Harbor Persp. Biol.* **2010**, *2*, a003574.
- (7) Fedor, M. *Annu. Rev. Biophys.* **2009**, *38*, 271.
- (8) Klawuhn, K.; Jansen, J. A.; Soucek, J.; Soukup, G. A.; Soukup, J. K. *ChemBioChem* **2010**, *11*, 2567.
- (9) Brooks, K. M.; Hampel, K. J. *Biochemistry* **2011**, *50*, 2424.
- (10) Emilsson, G. M.; Nakamura, S.; Roth, A.; Breaker, R. R. *RNA* **2003**, *9*, 907.
- (11) Klein, D. J.; Ferré-D'Amaré, A. R. *Science* **2006**, *313*, 1752.
- (12) Cochrane, J. C.; Lipchock, S. V.; Strobel, S. A. *Chem. Biol.* **2007**, *14*, 97.
- (13) Raines, R. T. *Chem. Rev.* **1998**, *98*, 1045.
- (14) McCown, P. J.; Roth, A.; Breaker, R. R. *RNA* **2011**, *17*, 728.
- (15) Roth, A.; Nahvi, A.; Lee, M.; Jona, I.; Breaker, R. R. *RNA* **2006**, *12*, 607.
- (16) Klein, D. J.; Been, M. D.; Ferré-D'Amaré, A. R. *J. Am. Chem. Soc.* **2007**, *129*, 14858.
- (17) Bevilacqua, P. C.; Brown, T. S.; Nakano, S.; Yajima, R. *Biopolymers* **2004**, *73*, 90.
- (18) Bevilacqua, P. C. *Biochemistry* **2003**, *42*, 2259.
- (19) Bevilacqua, P. C.; Yajima, R. *Curr. Opin. Chem. Biol.* **2006**, *10*, 455.
- (20) Wierchowski, J.; Wielgus-Kutrowska, B.; Shugar, D. *Biochim. Biophys. Acta* **1996**, *1290*, 9.
- (21) Da Costa, C. P.; Fedor, M. J.; Scott, L. G. *J. Am. Chem. Soc.* **2007**, *129*, 3426.
- (22) Liu, L.; Cottrell, J. W.; Scott, L. G.; Fedor, M. J. *Nat. Chem. Biol.* **2009**, *5*, 351.
- (23) Cottrell, J. W.; Scott, L. G.; Fedor, M. J. *J. Biol. Chem.* **2011**, *286*, 17658.
- (24) McCarthy, T. J.; Plog, M. A.; Floy, S. A.; Jansen, J. A.; Soukup, J. K.; Soukup, G. A. *Chem. Biol.* **2005**, *12*, 1221.
- (25) Cochrane, J. C.; Lipchock, S. V.; Smith, K. D.; Strobel, S. A. *Biochemistry* **2009**, *48*, 3239.
- (26) Klein, D. J.; Wilkinson, S. R.; Been, M. D.; Ferré-D'Amaré, A. R. *J. Mol. Biol.* **2007**, *373*, 178.
- (27) Wilkinson, S. R.; Been, M. D. *RNA* **2005**, *11*, 1788.
- (28) Brooks, K. M.; Hampel, K. J. *Biochemistry* **2009**, *48*, 5669.
- (29) Fedor, M. J. *Biochemistry* **1999**, *38*, 11040.
- (30) Li, Y.; Breaker, R. R. *J. Am. Chem. Soc.* **1999**, *121*, 5364.
- (31) Tinsley, R. A.; Furchak, J. R. W.; Walter, N. G. *RNA* **2007**, *13*, 468.
- (32) McClain, W. H.; Guerrier-Takada, C.; Altman, S. *Science* **1987**, *238*, 527.
- (33) Seela, F.; Jiang, D.; Xu, K. *Org. Biomol. Chem.* **2009**, *7*, 3463.
- (34) Soukup, G. A. *Nucleic Acids Res.* **2006**, *34*, 968.



- (35) Davis, J. H.; Dunican, B. F.; Strobel, S. A. *Biochemistry* **2011**, *50*, 7236.
- (36) Gong, B.; Klein, D. J.; Ferré-D'Amaré, A. R.; Carey, P. R. *J. Am. Chem. Soc.* **2011**, *133*, 14188.
- (37) Xin, Y.; Hamelberg, D. *RNA* **2010**, *16*, 2455.
- (38) Banás, P.; Walter, N. G.; Sponer, J.; Otyepka, M. *J. Phys. Chem. B* **2010**, *114*, 8701.
- (39) Dahm, S. C.; Derrick, W. B.; Uhlenbeck, O. C. *Biochemistry* **1993**, *32*, 13040.
- (40) Soukup, J. K.; Soukup, G. A. In *Non-protein Coding RNAs*; Walter, N. G., Woodson, S. A., Batey, R. T., Eds.; Springer-Verlag: Heidelberg, 2009; p 129.
- (41) Ferré-D'Amaré, A. R. *Q. Rev. Biophys.* **2010**, *43*, 423.
- (42) Rupert, P. B.; Ferré-D'Amaré, A. R. *Nature* **2001**, *410*, 780.
- (43) Jansen, J. A.; McCarthy, T. J.; Soukup, G. A.; Soukup, J. K. *Nat. Struct. Mol. Biol.* **2006**, *13*, 517.
- (44) Cochrane, J. C.; Strobel, S. A. *Acc. Chem. Res.* **2008**, *41*, 1027.
- (45) Soukup, G. A.; Breaker, R. R. *RNA* **1999**, *5*, 1308.
- (46) Min, D.; Xue, S.; Li, H.; Yang, W. *Nucleic Acids Res.* **2007**, *35*, 4001.
- (47) Chen, J. H.; Yajima, R.; Chadalavada, D. M.; Chase, E.; Bevilacqua, P. C.; Golden, B. L. *Biochemistry* **2010**, *49*, 6508.
- (48) Scott, L. G.; Tolbert, T. J.; Williamson, J. R. *Methods Enzymol.* **2000**, *317*, 18.
- (49) Hope, J. N.; Bell, A. W.; Hermodson, M. A.; Groarke, J. M. *J. Biol. Chem.* **1986**, *261*, 7663.
- (50) Switzer, R. L.; Gibson, K. J. *Methods Enzymol.* **1978**, *51*, 3.
- (51) Tolbert, T. J.; Williamson, J. R. *J. Am. Chem. Soc.* **1996**, *118*, 7929.
- (52) Scott, L. G.; Tolbert, T. J.; Williamson, J. R. In *RNA-Ligand Interactions Part A*; Abelson, J. N., Simon, M. I., Eds.; Methods in Enzymology 317; Academic Press: San Diego, CA, 2000; 18.
- (53) Geiser, M.; Cebe, R.; Drewello, D.; Schmitz, R. *Biotechniques* **2001**, *31*, 88.
- (54) Wang, W.; Malcolm, B. A. *Methods Mol. Biol.* **2002**, *182*, 37.
- (55) Milligan, J. F.; Uhlenbeck, O. C. *Methods Enzymol.* **1989**, *180*, 51.
- (56) Urrutia, R.; McNiven, M. A.; Kachar, B. *J. Biochem. Biophys. Methods* **1993**, *26*, 113.
- (57) Lincoln, T. A.; Joyce, G. F. *Science* **2009**, *323*, 1229.
- (58) DeLano, W. L. *The PyMOL Molecular Graphics System*; DeLano Scientific LLC: San Carlos, CA, 2004.